ACS chemical biology

Articles

pubs.acs.org/acschemicalbiology

Design of a Cyclotide Antagonist of Neuropilin-1 and -2 That Potently Inhibits Endothelial Cell Migration

Jennifer A. Getz,[†] Olivier Cheneval,[‡] David J. Craik,[‡] and Patrick S. Daugherty*,[†]

[†]Department of Chemical Engineering, University of California, Santa Barbara, California 93106, United States

[‡]Institute for Molecular Bioscience, The University of Queensland, Brisbane, QLD 4072, Australia

Supporting Information

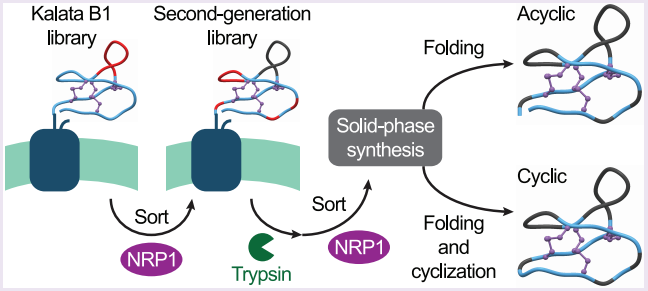

ABSTRACT: Neuropilin-1 and -2 are critical regulators of angiogenesis, lymphangiogenesis, and cell survival as receptors for multiple growth factors. Disulfide-rich peptides that antagonize the growth factor receptors neuropilin-1 and neuropilin-2 were developed using bacterial display libraries. Peptide ligands specific for the VEGFA binding site on neuropilin-1 were identified by screening a library of disulfide-rich peptides derived from the thermostable, protease-resistant cyclotide kalata B1. First generation ligands were subjected to one cycle of affinity maturation to yield acyclic peptides with affinities of 40−60 nM and slow dissociation rate constants ($\sim 1 \times 10^{-3}$ s^{-1}). Peptides exhibited equivalent affinities for human and mouse neuropilin-1 and cross-reacted with human neuropilin-2 with lower affinity. A C-to-N cyclized variant (cyclotide) of one neuropilin ligand retained high affinity, exhibited increased protease resistance, and conferred improved potency for inhibiting endothelial cell migration *in vitro* ($EC_{50} \approx 100$ nM). These results demonstrate that potent, target-specific cyclotides can be created by evolutionary design and that backbone cyclization can confer improved pharmacological properties.

The receptors neuropilin-1 (NRP1) and neuropilin-2 (NRP2) serve critical roles in normal vascular and lymphatic development. However, these receptors are also implicated in pathological angiogenesis and cell survival in human cancers. Neuropilins interact with a surprising number of growth factors known to promote angiogenesis and tumor progression, including VEGFs and HGF for NRP1 and NRP2, and PIGF, FGF, and PDGF for NRP1.[1] NRP1 not only enhances the interaction of VEGF with its receptors[2,3] but also serves as an independent receptor for multiple VEGF isoforms. High levels of NRP1 expression on glioma, metastatic breast, pancreatic, and colon cancer cells has been proposed to promote tumor cell survival and chemoresistance through autocrine signaling loops.[4−7] For example, NRP1 expression on pancreatic cancer cells increases HGF-mediated cell invasion through interaction with c-Met and also increases cell survival in glioma cells.[5,8] In addition to growth factor mediated signaling, the extracellular domain of NRP1 has been shown to interact with the epidermal growth factor receptor to enhance AKT signaling upon EGF or TGFα interaction.[9] These studies indicate that the role of NRP1 in promoting tumor progression and survival extends beyond a pro-angiogenic role.

Blockade of neuropilins has been shown to enhance the efficacy of cancer therapeutic agents through multiple distinct mechanisms. Anti-NRP1 antibodies have an additive effect in reducing tumor growth when delivered with an anti-VEGF antibody by blocking vascular remodeling and endothelial cell migration.[10] Despite preclinical efficacy of the anti-NRP1 antibody, atypically fast serum clearance was observed in mice due to saturation of receptors on non-target tissues, as well as faster non-specific clearance in humans compared to other human monoclonal antibodies.[11,12] A peptide named iRGD interacts with both integrins and NRP1 via a C-terminal $RGD^{K}/_{R}$ motif and increased the tumor penetration and efficacy of co-administered chemotherapeutic agents and monoclonal antibodies.[13,14] Instead of inhibiting angiogenesis mediated through NRP1, an antibody that blocks NRP2 decreased tumor lymphangiogenesis and reduced metastasis to lymph nodes.[15] Collectively, these previous studies suggest that potent neuropilin antagonists, which combine dual specificity with efficient tumor penetration, could enhance the efficacy of anti-neuropilin agents for cancer therapy.

Disulfide-rich peptides can confer high receptor binding affinity and intrinsic resistance to proteolytic enzymes, thereby

Received: January 24, 2013
Accepted: March 28, 2013
Published: March 28, 2013

   dx.doi.org/10.1021/cb4000585 | *ACS Chem. Biol.* 2013, 8, 1147−1154

making them attractive alternatives to antibodies for therapeutic development. In particular, C-to-N cyclized peptides (cyclotides) frequently possess superior chemical and proteolytic stability properties for *in vivo* use.[16] Both knottins and cyclotides possess an extensive hydrogen bonding network and a characteristic cystine knot motif. The knot is formed by three disulfide bonds; two of the bonds create a ring with the peptide backbone through which the third disulfide bond passes. The binding specificity of the naturally occurring cyclotide kalata B1 has been redirected toward several protein targets, yielding peptide ligands with substantially improved proteolytic resistance. For example, the screening of a kalata B1-based peptide library yielded thrombin inhibitors with resistance to the digestive proteases trypsin and chymotrypsin.[17] Orally available bradykinin B_1 receptor antagonists were developed by grafting the appropriate ligand sequence into the kalata B1 scaffold, and the resulting molecule induced a significant analgesic effect in mice.[18] Kalata B1 also was engineered as a high-affinity, specific melanocortin agonist.[19] Here we used the kalata B1 scaffold as a template, along with bacterial display, to create and affinity mature a potent cyclotide inhibitor of NRP1 and NRP2 (Figure 1). Comparison of the

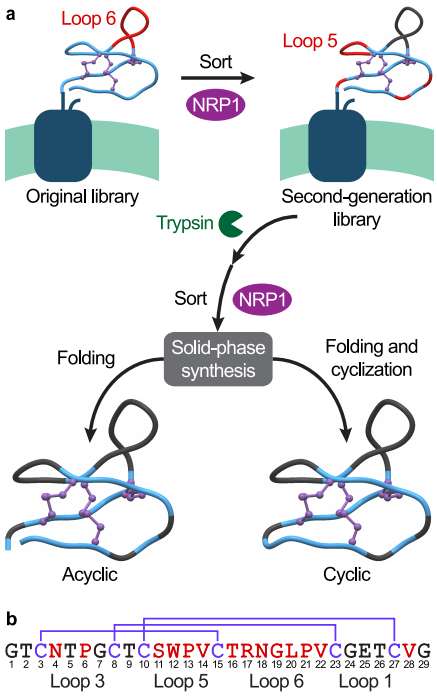

Figure 1. Cyclotide ligand design strategy. (a) Concept figure showing the two kalata B1-based libraries with the randomized positions highlighted in red, fixed regions in black, and the final synthesis of the acyclic and cyclic ligands. (b) Peptide sequence of kalata B1 with the positions that were mutated in the final NRP1 ligands shown in red, the six cysteines in purple, and the native disulfide connectivity.

function-blocking effect of the cyclotide with the otherwise identical acyclic peptide from which it derives provided evidence that the cyclotide has superior biological efficacy.

RESULTS AND DISCUSSION

Discovery of NRP1 Ligands from a Kalata B1 Library. To identify stable, high-affinity cyclic ligands specific for NRP1, a bacterial display library of disulfide-rich peptides, derived from the kalata B1 scaffold, was screened against the NRP1 extracellular domain. The library was constructed by randomizing seven residues within loop 6 of the cyclotide kalata B1 and contained ~6×10^9 members.[17] Sequential rounds of MACS and FACS were used to enrich the library for high-affinity clones. Isolated NRP1-binding clones were grouped into three consensus families: $Q^L/_M ARG^K/_A{}^V/_K$, $KP^V/_A R^G/_S{}^V/_L{}^R/_K$, and $K^A/_V PR^M/_G{}^L/_V{}^R/_K$ (Table 1). The first position of the

Table 1. Sequences of NRP1 Binding Peptides[a]

Name	Sequence
	Kalata B1 Library
Library Design	GTCNTPGCTCSWPVC**TRNGLPV**CGETCVG
N1.1	GTCNTPGCTCSWPVC**QIVRGAR**CGETCVG
N1.2	GTCNTPGCTCSWPVC**QMVRGAK**CGETCVG
N1.3	GTCNTPGCTCSWPVC**QVARMNV**CGETCVG
N1.4	GTCNTPGCTCSWPVC**QLARGKV**CGETCVG
N1.5	GTCNTPGCTCSWPVC**QLARGKV**CGETCVG
N1.6	GTCNTPGCTCSWPVC**GPAPRKL**CGETCVG
N1.7	GTCNTPGCTCSWPVC**AMRGVVK**CGETCVG
Consensus	**$Q\text{-}^L/_M\text{-}A\text{-}R\text{-}G\text{-}^K/_A\text{-}^V/_K$**
N1.8	GTCNTPGCTCSWPVC**KPVRSVK**CGETCVG
N1.9	GTCNTPGCTCSWPVC**KPARGLR**CGETCVG
N1.10	GTCNTPGCTCSWPVC**KPVRGVR**CGETCVG
Consensus	**$K\text{-}P\text{-}^V/_A\text{-}R\text{-}^G/_S\text{-}^V/_L\text{-}^R/_K$**
N1.11	GTCNTPGCTCSWPVC**RLPRGLK**CGETCVG
N1.12	GTCNTPGCTCSWPVC**KGPRMLK**CGETCVG
N1.13	GTCNTPGCTCSWPVC**KAPRMVG**CGETCVG
N1.14	GTCNT**S**GCTCSWPVC**KAPRMVR**CGETCVG
N1.15	GTCNTPGCTCSWPVC**KVPRVVR**CGETCVG
N1.16	GTCNTPGCTCSWPVC**KVPRGAR**CGETCVG
N1.17	GTCNTPGCTCSWPVC**KVPRGLR**CGETCVG
Consensus	**$K\text{-}^A/_V\text{-}P\text{-}R\text{-}^M/_G\text{-}^L/_V\text{-}^R/_K$**
	Second-Generation Library
Library Design	GTC**NTP**GCTC**SWPV**CKAPRMVRCGETC**VG**
N2.1	GTC**RTF**GCTC**KPLR**CKAPRMVRCGETC**MG**
N2.2	GTC**STL**GCTC**KPLR**CKAPRMVRCGETC**GG**
N2.3	GTC**STL**GCTC**KPPR**CKAPRMVRCGETC**LG**
Consensus	**S L KPLR X**
N2.4	GTC**RTW**GCTC**MPLR**CKAPRMVRCGETC**EG**
N2.5	GTC**STG**GCTC**LPLR**CKAPRMGRCGETC**TG**
N2.6	GTC**RTL**GCTC**LPVR**CKAPRMVRCGETC**WG**
N2.7	GTC**RTG**SCTC**FLPR**CKAPRMVRCGETC**EG**
N2.8	GTC**RTV**GCTC**SWTR**CKAPRMVRCGETC**DG**
Consensus	**R X XPXR X**
N2.9	GTC**STR**GCTC**TFRK**CKAPRMVRCGETC**CG**
N2.10	GTC**STV**GCTC**TVIP**CKAPRMVRCGETC**EG**
N2.11	GTC**NTG**GCTC**MDSTC**MAPRMVRCGETC**GG**
N2.12	GTC**STM**GCTC**PRIP**CKAPRM**G**RCGETC**SG**
Consensus	**S X TXXP X**
N2.13	GTC**KPVR**CKAPRMVRCGETCGG

[a]The randomized positions from each library are shown in bold black. Positively charged residues (arginine and lysine) are highlighted in gray.

randomized region strongly preferred lysine and glutamine considering these amino acids are encoded by a single codon using the NNS scheme versus the three codons that encode arginine. Arginine was highly conserved at the fourth position with almost exclusively hydrophobic amino acids (L, V, A, P) between the conserved arginine and lysine residues. Arginine and lysine were preferred in the seventh position of loop 6, which is the end of a disulfide-constrained loop within the kalata B1 scaffold. Thus, the free C-terminal carboxyl group of R or K, previously reported to be critical for high-affinity

dx.doi.org/10.1021/cb4000585 | *ACS Chem. Biol.* 2013, 8, 1147–1154

binding to NRP1,[20] was not required. The majority of first-generation peptide sequences possessed apparent equilibrium dissociation constants of 100−200 nM for NRP1, as measured using flow cytometry (Supplementary Figure 1). The peptides also bound with similar affinity to mouse NRP1 (data not shown), which shares >90% identity with human NRP1.[21]

In order to verify that the NRP1-binding peptides recognized the endogenous receptor on cells, the binding of peptide-displaying fluorescent bacterial clones to NRP1-expressing tumor cells was measured using flow cytometry. Three NRP1 ligands selected from different consensus groups (N1.1, N1.8, N1.14) each bound effectively to NRP1-expressing PPC-1 prostate cancer and MDA-MB-231 breast cancer cells[3,22] (Figure 2, Supplementary Figure 2). In contrast, the bacteria

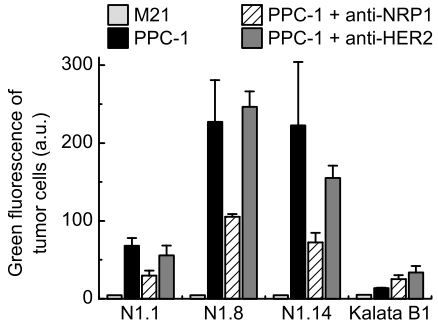

Figure 2. Peptide-displaying bacteria bind specifically to NRP1-expressing cells. Binding of green fluorescent bacteria displaying the NRP1 ligands to M21 melanoma cells (light gray), PPC-1 prostate cancer cells (black), PPC-1 cells preincubated with an anti-NRP1 polyclonal antibody (diagonal lines), and PPC-1 cells preincubated with a HER2-specific monoclonal antibody (dark gray). The error bars represent the standard deviation of duplicate samples.

did not bind to M21 melanoma cells, which express VEGFR1 and VEGFR2, but not NRP1.[22,23] Preincubation of the PPC-1 cells with the anti-NRP1 polyclonal antibody decreased the binding signal between the tumor cells and the ligand-displaying bacteria by 45−60%, whereas an unrelated anti-HER2 monoclonal antibody did not inhibit binding. Furthermore, native *E. coli* surface proteins and the kalata B1 display scaffold did not substantially contribute to the binding since bacteria displaying the native kalata B1 sequence did not bind appreciably to the tumor cell lines. Binding was not completely blocked by the anti-NRP1 antibody, suggesting the peptides may also interact with related receptors such as NRP2[3] or that the polyclonal antibody does not completely block the peptide-binding site. For example, previous work with a neuropilin peptide ligand (CGNKRTR) demonstrated that the binding to DU145 cells, which express NRP1 but not NRP2, was also incompletely inhibited by a 3-fold greater concentration of the same polyclonal anti-NRP1 antibody used in this work.[24] In addition, this neuropilin-binding peptide also exhibited binding to endogenous NRP2 receptors expressed on MDA-MB-435 cells.

With the goal of enhancing the affinity and aqueous solubility of the first-generation NRP1 ligands, a second-generation bacterial display peptide library was constructed and screened (Figure 1, Figure 3a). Four hydrophobic residues in loop 5 (SWPV), along with P6 and V28, were fully randomized (Table 1), while the neuropilin-binding epitope of N1.14 (KAPRMVR) was fixed in loop 6. In addition, N4 was partially randomized (to R/K/N/S) to allow for the possibility of scaffold stabilization through a salt bridge with E25 that would constrain the N- and C-termini in close proximity to mimic the circular backbone of native kalata B1. Sorting the second-generation library with reduced NRP1 concentrations (10−30 nM) and exposing the library populations to an excess of trypsin favored high-affinity and protease-resistant ligands.[17] Screening enriched a population of peptides that, unlike the parental peptide N1.14, exhibited high affinity before and after treatment with trypsin. Sequencing identified 12 unique full-length NRP1-binding peptides (Table 1) and a highly represented peptide fragment with four cysteines (N2.13). The first consensus group contained an additional KxxR motif within loop 5 ($KP^{L}/_{P}R$), and the second consensus group had hydrophobic residues in the first three positions of loop 5 and a conserved arginine in the fourth position (e.g., LPLR). Three of the five peptides in the second group exhibited both N4R and V28E/D, suggesting that this substitution pair might stabilize the acyclic scaffold. Overall, peptides from the second generation library exhibited higher binding responses at lower NRP1 concentrations and increased binding after trypsin treatment (Figure 3b).

Previous studies have demonstrated that peptides exhibiting a free C-terminal arginine or lysine residue bind with substantially increased affinity to NRP1. Consequently, the C-terminal R/KxxR/K motif was dubbed the C-end rule (CendR).[22] In contrast to these previous reports, the disulfide-rich NRP1 binding peptides identified here do not possess a C-terminal arginine residue.[22] Molecular modeling suggested that tight backbone turns enabled by a glycine

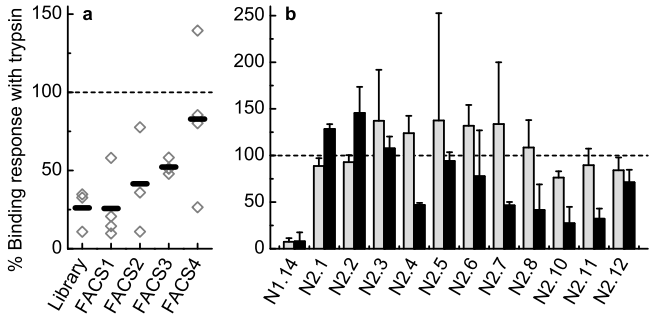

Figure 3. Trypsin resistance of cell-surface displayed peptides. (a) Each successive round of sorting of the second-generation library increased the trypsin-resistance of the displayed peptides. (b) Individual clones were assayed by flow cytometry after treatment with 2 μM trypsin and normalized to the signal without trypsin. Two different induction conditions (with EDTA in light gray and without EDTA in black) were used to determine if increasing the peptide display level would alter trypsin resistance. The error bars represent the standard deviation of triplicate samples.

dx.doi.org/10.1021/cb4000585 | *ACS Chem. Biol.* 2013, 8, 1147−1154

residue immediately following R/K (i.e., RxxKxxRG) can allow effective peptide docking into the NRP1 B1 domain pocket.[20] In a similar fashion, the disulfide bond formed by the cysteine following R/K in the kalata B1 scaffold may enable the final arginine in loop 6 to dock tightly into the pocket in the NRP1 B1 domain, thereby obviating the need for a free carboxyl terminus to enable a high-affinity interaction.[20] Unlike the iRGD peptide, which required cleavage following an arginine residue for binding to NRP1,[24] proteolytic cleavage of the kalata B1-based peptides was not required to activate binding function.

Synthesis and Characterization of NRP1 Ligands. Synthetically prepared acyclic peptides were oxidatively folded using immobilized Ellman's reagent, whereas the cyclic peptides were generated using a one-pot cyclization and oxidation reaction. Following purification of the peptides with RP-HPLC, mass spectrometry measurements verified that the peptides contained three disulfide bonds. The purified material may have contained multiple species with differing disulfide connectivities due to co-elution of these species in a single HPLC peak. Unlike the NRP1-binding cyclotide, cyclic kalata B1 with the correct disulfide connectivity elutes during purification as a sharp, distinct, and hydrophobic peak separate from any misfolded material. Therefore, the synthesized and purified parent kalata B1 molecule contained a single, native structure as has been previously confirmed using NMR.[25] Since the neuropilin ligands were generated by mutating approximately 50% of the amino acids in the original peptide scaffold, overall structures and folding yields of the ligands differed from those of the parental scaffold.

Affinity-matured acyclic peptides (N2.1, N2.2, N2.6) bound human NRP1 with K_D values of 40−60 nM and exhibited slow dissociation constants of 1×10^{-3} s^{-1} (Figure 4, Table 2). The

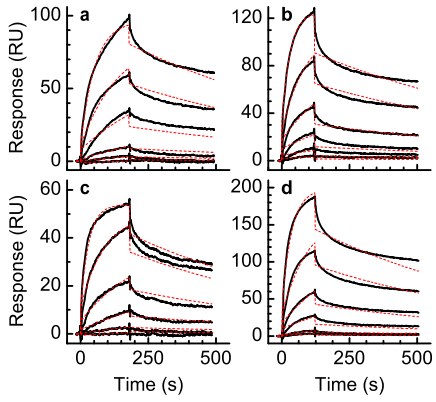

Figure 4. Binding kinetics of the kalata B1-based ligands with human NRP1. Binding responses for a concentration series from 4.1 nM to 1 μM of (a) N2.1, (b) cyclic N2.1C, (c) N2.2, and (d) N2.6 were measured using surface plasmon resonance (SPR) with surface-immobilized human NRP1. The raw data (black lines) were fit with a 1:1 Langmuir binding model (dashed red lines).

cyclized form of N2.1 (N2.1C) also exhibited affinity and binding kinetics equivalent to those of the acyclic peptide. Although the curves were fit to a 1:1 Langmuir model, the dissociation phases appeared biphasic and were therefore also fit to a biexponential model (Supplementary Figure 3). For both N2.1 and N2.1C, approximately 75% of the material dissociated with a slower off-rate (6×10^{-4} s^{-1}), while 25% of the material had an off-rate 50-fold faster (3×10^{-2} s^{-1}). The disulfide-rich kalata B1 scaffold contributed substantially to the binding affinity of the NRP1 ligands. The 7-mer peptide KAPRMVR present within N1.14 had an equilibrium binding affinity of approximately 10 μM for human NRP1 (Supplementary Figure 4), demonstrating that the scaffold provided a roughly 200-fold improvement in affinity. Each of the peptides characterized exhibited equivalent affinities for human and mouse NRP1 (Table 2, Supplementary Figure 5). The peptides also bound human NRP2, albeit with reduced affinity. The binding interactions of cyclic and acyclic N2.1 with human NRP2, when compared to the binding interactions with NRP1, exhibited 3-fold slower association rates ($7.2–9.8 \times 10^4$ $M^{-1}s^{-1}$ versus $2.2–3.1 \times 10^4$ $M^{-1}s^{-1}$) and 2-fold faster dissociation rates (2.1×10^{-3} s^{-1} versus 1×10^{-3} s^{-1}) (Supplementary Figure 6). Also, the parent scaffold, cyclic kalata B1, did not exhibit measurable affinity for human NRP1, mouse NRP1, or human NRP2.

The affinities of the neuropilin ligands developed here are nearly 2 orders of magnitude higher than previously discovered ligands harboring the KxxR motif. The peptides RPARPAR and iRGD have reported K_D values of ~2 μM.[14,22] Moreover, the NRP1 ligands reported here exhibit dissociation rate constants of 1×10^{-3} s^{-1}, which is comparable to a first-generation function-blocking anti-NRP1 monoclonal antibody.[26] Increased residence time for the receptor−ligand complex would be expected to improve the retention and therapeutic effect of the ligand. The biexponential dissociation kinetics observed here may have resulted from the presence of multiple distinct disulfide conformers co-eluting together; this co-elution has been previously observed for peaks containing misfolded kalata B1.[27] The improved affinity of the NRP1 ligands is due in part to the repeated KxxR binding motif in loops 5 and 6 and the additional constraints conferred by the three disulfide bonds of the kalata B1 scaffold. The repeated epitope may bind to two distinct sites on NRP1 or alternatively bind to the same site on NRP1 with a higher effective concentration of the interaction epitope. Regardless of the mechanism, the increased affinity of these novel cyclotide NRP1/2 ligands provides an opportunity to investigate the effect of neuropilin blockade on tumor progression.

Cyclotide N2.1C exhibits dual specificity for human NRP1 and NRP2, a characteristic that would be expected to improve antitumor efficacy. The preferential specificity of $VEGFA_{165}$ for the B1B2 domain of NRP1 over that of NRP2 has been attributed to the negatively charged exon 7 encoded domain of $VEGFA_{165}$ that repels a similarly negatively charged loop on NRP2, which is not present on NRP1.[28] This electrostatic repulsion is responsible for the 50-fold higher affinity that $VEGFA_{165}$ has for NRP1 compared to that for NRP2. The peptide ligands here mimic exon 8 of $VEGFA_{165}$ and do not have a negatively charged patch, so this electrostatic repulsion should not occur. Although NRP1 and NRP2 share an overall sequence identity of only 47%, the regions that interact with exon 8 of $VEGFA_{165}$ are somewhat conserved.[3] Additionally, RPARPAR binds to NRP2, but with lower affinity than to NRP1. Interestingly, phage displaying a RPARPAR-like motif were internalized into MDA-MB-435 breast carcinoma cells that express NRP2, but not NRP1.[24] The interaction of the second-generation ligands with NRP2 may explain the partial decrease in binding response of bacteria displaying neuropilin-binding peptides when the tumor cells were preincubated with an anti-NRP1 antibody. Therefore, the reduced affinity of the peptide ligands for NRP2 is consistent with previous studies,

dx.doi.org/10.1021/cb4000585 | ACS Chem. Biol. 2013, 8, 1147−1154

Table 2. Parameters for the Binding Kinetics of the NRP1 Ligands with Human and Mouse NRP1[a]

ID	k_a (M^{-1} s^{-1})	k_d (s^{-1})	K_D (nM)	R_{max} (RU)
		Human NRP1		
N2.1	$2.2 \pm 1.0 \times 10^4$	$1.09 \pm 0.07 \times 10^{-3}$	56 ± 23	100 ± 11
N2.1C	$2.7 \pm 0.4 \times 10^4$	$1.4 \pm 0.3 \times 10^{-3}$	51 ± 15	75 ± 19
N2.2	$3.1 \pm 0.5 \times 10^4$	$1.28 \pm 0.02 \times 10^{-3}$	42 ± 6	61 ± 16
N2.6	$3.7 \pm 2.1 \times 10^4$	$1.1 \pm 0.3 \times 10^{-3}$	34 ± 15	157 ± 57
		Mouse NRP1		
N2.1	$2.1 \pm 0.8 \times 10^4$	$1.1 \pm 0.1 \times 10^{-3}$	59 ± 35	122 ± 41
N2.1C	$2.7 \pm 0.3 \times 10^4$	$1.4 \pm 0.2 \times 10^{-3}$	52 ± 12	103 ± 25
N2.2	$2.4 \pm 0.5 \times 10^4$	$1.5 \pm 0.2 \times 10^{-3}$	67 ± 22	72 ± 25
N2.6	$2.0 \pm 0.3 \times 10^4$	$1.1 \pm 0.2 \times 10^{-3}$	54 ± 9	320 ± 91

[a]The uncertainties represent the standard deviation from triplicate measurements.

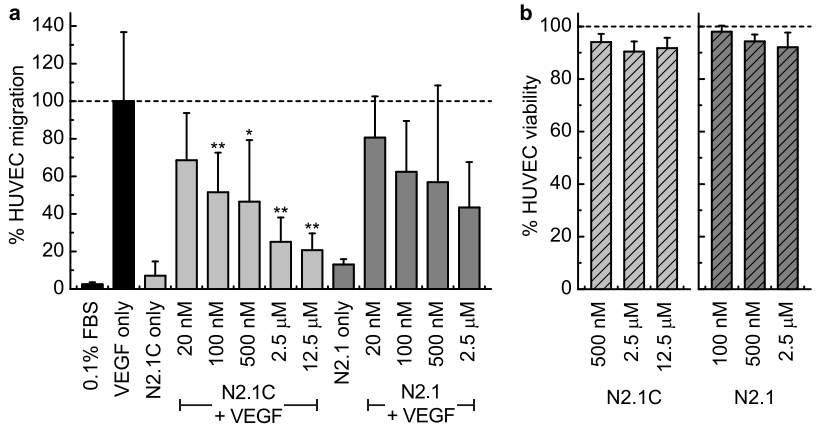

Figure 5. HUVEC migration and viability assays. (a) A 5-fold concentration series of either N2.1C or N2.1 was preincubated with the HUVECs followed by the addition of 3.3 nM $VEGFA_{165}$ to determine if the NRP1 ligand could inhibit migration. The peptides alone (500 nM) did not alter the extent of migration. The error bars represent the standard deviation from six inserts for cyclic N2.1C and three inserts for acyclic N2.1. A one-sided Mann–Whitney test was used to assess statistical significance in the migration difference between the VEGF only control and cells incubated with N2.1C (significance levels: * $\alpha = 0.05$, ** $\alpha = 0.01$). The overall extent of migration was between 35 and 110 HUVECs per field of view for the VEGF only condition in separate experiments, and the data were normalized to this condition. (b) HUVECs showed over 90% viability following incubation with either N2.1C or N2.1. The error bars represent the standard deviation from triplicate wells.

and the interaction with NRP2 may increase the efficacy of the ligands.

To assess the suitability of these cationic NRP1-binding peptides for use in cell culture and *in vivo* studies, their cytotoxicity toward PPC-1, M21, and MDA-MB-231 cell lines was measured. Peptide N2.1 and the corresponding cyclotide N2.1C did not exhibit measurable toxicity against any of the cell lines (Supplementary Figure 7). However, peptides N2.2 and N2.6 exhibited mild toxicity toward one of three tumor cell lines at the highest concentration tested: 65–75% of the M21 melanoma cells were viable after a 24 h incubation with 10 μM N2.2 and N2.6. All of the four peptides assayed were nontoxic toward PPC-1 and MDA-MB-231 cells, while the control peptide melittin (+6 net charge at physiological pH) exhibited toxicity levels similar to that previously reported (IC_{50} of 1–2 μM, Supplementary Figure 8).[29] Toxicity of melittin, N2.2, and N2.6 occurred independently of NRP1 expression. M21 cells express negligible levels of NRP1, while PPC-1 and MDA-MB-231 cells express high levels of the receptor.

Because the second-generation NRP1/2 ligands are highly cationic, electrostatic attraction of the peptides to the negative charge on cell membranes could lead to potential cytotoxicity due to disruption of the lipid bilayer. At physiological pH, peptides N2.1 and N2.1C both carry an overall charge of +5. Cyclotide N2.1C, however, was nontoxic to multiple tumor cell lines unlike the cationic bee venom peptide melittin. For comparison, cyclotides MCoTI-II and kalata B1 are internalized into tumor cells through both electrostatic and hydrophobic interactions with the lipid membrane, and kalata B1 was cytotoxic at concentrations above 5 μM.[30] In the second-generation library, the hydrophobic residues within the kalata B1 scaffold were randomized to increase the solubility of the peptides. By substituting the hydrophobic amino acids, the peptides became less amphiphilic since the remaining hydrophobic residues were surrounded by positively charged, hydrophilic amino acids. Without the hydrophobic, solvent-exposed patch, the NRP1-binding peptides apparently can no longer bury into and disrupt the lipid membrane of cells. Given that N2.1 and N2.1C were nontoxic and bound NRP1 with high affinity, these ligands were chosen for further characterization in biological assays.

NRP1-Binding Cyclotide Inhibits HUVEC Migration. Since neuropilin blockade has been previously shown to inhibit VEGF-stimulated endothelial cell migration, a Boyden chamber assay was performed to assess the extent to which the peptides N2.1 and N2.1C inhibited human umbilical vein endothelial cell (HUVEC) migration. Cyclotide N2.1C potently inhibited VEGF-stimulated migration of HUVECs, exhibiting an EC_{50} of ~100 nM (Figure 5a). Migration was strongly inhibited by up to 80% at a N2.1C concentration of 12.5 μM. The acyclic

dx.doi.org/10.1021/cb4000585 | *ACS Chem. Biol.* 2013, 8, 1147–1154

peptide N2.1 also inhibited HUVEC migration, but with reduced potency. The peptides did not substantially reduce HUVEC viability under conditions identical to those of the migration assay (Figure 5b). Thus, cyclotide N2.1C was a potent antagonist of NRP1 and NRP2 and blocked $VEGFA_{165}$ from interacting with NRP1.

To investigate whether the increased potency of the cyclotide was due to increased proteolytic resistance, the stability of N2.1 and N2.1C was measured against three endopeptidases frequently activated in human solid tumors:[31,32] urokinase-type plasminogen activator (uPA), matriptase-1 (MT-SP1), and matrix metalloproteinase 9 (MMP-9). None of the tumor-associated proteases degraded the parental cyclic kalata B1 molecule after 6-h digestions (Figure 6). Cyclotide N2.1C exhibited increased resistance to both uPA and MMP-9 when compared to the acyclic N2.1 but was more susceptible to MT-SP1. The major products of the degradation of acyclic N2.1 by MT-SP1 were the full-length peptide with a single cut, as well as two peptide fragments that resulted from hydrolysis following R19 in loop 6 (Supplementary Figure 9). For the cyclotide N2.1C, the major degradation product of MT-SP1 digestion was the full-length peptide with a single cut. The once-cut cyclotide may retain its binding activity because it remains full length, while the acyclic peptide is digested into two fragments.

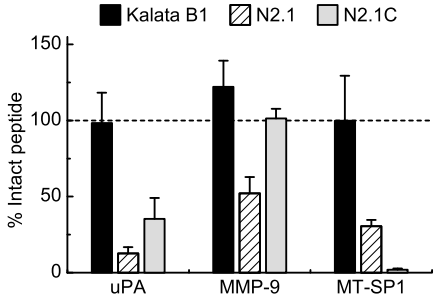

Figure 6. Protease stability of acyclic versus cyclic peptides. Cyclic kalata B1, N2.1, and N2.1C were exposed to 200 nM uPA, 200 nM MMP-9, and 20 nM MT-SP1 for 6 h. The cyclic peptide N2.1C had increased stability with uPA and MMP-9 compared to the acyclic peptide N2.1 but was degraded more rapidly by MT-SP1. The error bars represent the standard deviation from triplicate experiments.

Both N2.1 and N2.1C inhibited the $VEGFA_{165}$-mediated migration of HUVECs, with the cyclotide demonstrating a higher potency relative to the acyclic variant. This increased potency may result from increased resistance to proteases including uPA and MMP-9, both of which are expressed by HUVECs.[33,34] Interestingly, the EC_{50} of N2.1C for inhibition of HUVEC migration (100 nM) was within 2-fold of the K_D of the peptide for NRP1, even though HUVECs express other VEGF receptors (VEGFR1 and VEGFR2) in addition to NRP1 and NRP2. The previously reported NRP1 ligand, EG3287, blocked $VEGFA_{165}$ binding to porcine aortic cells expressing NRP1 with an IC_{50} of 2.8 μM (K_i of 1.2 μM).[35] Binding of $VEGFA_{165}$ to MDA-MB-231 breast cancer cells, which express NRP1 but not VEGFR2, was also inhibited by EG3287 at a similar IC_{50}. However, EG3287 demonstrated reduced efficacy when inhibiting the binding of $VEGFA_{165}$ to HUVECs (IC_{50} of 20 μM) due to the presence of additional VEGF receptors. In contrast, the high-affinity cyclotide N2.1C exhibited potent inhibition of HUVEC migration despite the presence of additional VEGF receptors. These results suggest that the cyclotide blocks the interaction of the VEGFR2-VEGF complex with NRP1 to inhibit endothelial cell migration.

Cyclotide N2.1C, exhibiting improved affinity and dual specificity, coupled with a small size and increased protease resistance, provides a new tool to investigate the roles of neuropilins in pathological processes *in vivo*. More generally, the screening and affinity maturation strategy described here provides a new route to create small, stable bioactive ligands with properties intermediate between small molecules and antibodies that may be useful for diagnostic and therapeutic applications.

METHODS

Sorting the Kalata B1 Library against NRP1. The human NRP1 extracellular domain (aa F22–K644, R&D Systems) was biotinylated and used for sorting. A bacterial display peptide library containing ~6×10^9 variants of kalata B1 was subcultured 1:50 into LB with 34 μg mL^{-1} chloramphenicol and grown at 37 °C for 2 h.[17] Expression was induced for 1 h at 37 °C by the addition of 0.04% w/v arabinose. Peptide ligands for NRP1 were enriched using one round of MACS with 100 nM biotinylated NRP1 followed by four rounds of FACS with NRP1 concentrations of 100 nM for two rounds, 50 nM for the third round, and 25 nM for the final round.[36] The cells were washed and labeled with 17 nM streptavidin-phycoerythrin (SAPE; Invitrogen) prior to FACS. To prevent the enrichment of streptavidin-binding peptides, the bacterial population was first incubated with streptavidin-coated magnetic beads using a bead:cell ratio of 1:1, and streptavidin-bound bacteria were removed prior to the incubation of the library population with NRP1. Plasmid DNA isolated from individual clones obtained in the third and fourth rounds of FACS was submitted for sequencing.

Binding of Displayed NRP1 Ligands to Tumor Cells. To demonstrate specificity of the displayed peptides for native NRP1, the peptides were cloned into the GFP-eCPX plasmid,[37] and individual clones were assayed for their ability to bind two tumor cell lines: PPC-1 (high NRP1) and M21 (low NRP1).[22] Tumor cells were scraped from the tissue culture plate (~5×10^5 tumor cells per sample) and washed once with PBS. Bacteria were then incubated with the tumor cells for 1 h at 4 °C at a ratio of 50 bacteria per tumor cell (2.5×10^7 bacterial cells per sample). The mean green fluorescence (530 nm) of the tumor cells was measured using flow cytometry. For the competition assay, the tumor cells were first incubated with 200 nM of either the polyclonal goat anti-NRP1 antibody (R&D Systems) or the control anti-HER2 antibody for 1 h at 4 °C followed by the addition of the bacteria.

Affinity Maturation of NRP1-Binding Peptides. In a second-generation library, the NRP1-binding epitope from peptide N1.14 (KAPRMVR) was fixed in loop 6 of the kalata B1 scaffold, and mutations were introduced within the surrounding scaffold residues. N4 was mutated using codon ARN to enable R/K/N/S residues at that position. P6, S11–V14 (loop 5), and V28 were completely randomized with NNS codons. The library was constructed using the primers in Supplementary Table 1 following a published protocol[38] and contained ~4×10^6 independent transformants.

To favor the collection of cells displaying peptides with improved affinity and protease resistance, cells were exposed to trypsin at concentrations that degraded sensitive peptides but did not compromise cell viability. To verify that the bacterial display system was compatible with trypsin exposure, bacterial clones displaying either a trypsin-sensitive streptavidin binder (AECHPQGPPCIEGR↑K↑)[39] or an insensitive peptide (anti-T7Mab tag: MASMTGGQQ-MG) were assayed for binding to their reporters before and after trypsin exposure. Approximately 10^8 cells were pelleted and resuspended in 50 μL of trypsin solution. Bacteria were incubated with trypsin for 30 min at 37 °C prior to addition of the target protein, and a range of trypsin concentrations (16 nM–2 μM) was tested to identify the protease concentration yielding >90% streptavidin binder

dx.doi.org/10.1021/cb4000585 | *ACS Chem. Biol.* 2013, 8, 1147–1154

cleavage without T7 tag cleavage. Following the trypsin digestion, the streptavidin binder and T7 tag clones were labeled with either 100 nM SAPE or with 13 nM biotinylated anti-T7 antibody (EMD Chemicals) followed by 17 nM SAPE. With trypsin concentrations of 400 nM and 2 μM, the fluorescence of the positive control decreased to the background level, while the negative control maintained a constant level of fluorescence (Supplementary Figure 10). To ensure that the eCPX scaffold was not degraded by trypsin, the substitution K6N was introduced by site-directed mutagenesis. Again, the streptavidin binder displayed using eCPX K6N was rapidly degraded by trypsin, while the T7 tag clone was resistant up to 250 μM trypsin.

Sorting of a second-generation library was performed as described above with the addition of an incubation step with 400 nM trypsin for 30 min before the first two rounds and 2 μM trypsin for the last two rounds. Following trypsin incubation, the cells were washed with cold PBS and incubated with 30 nM NRP1 for the first three rounds and 10 nM NRP1 for the last round. DNA sequencing of clones from the third and fourth rounds of sorting revealed 12 full-length sequences and a highly represented truncated peptide with four cysteines (N2.13). Individual clones were assayed for binding after exposure to 2 μM trypsin and labeling with 100 nM NRP1. To enhance the display of these disulfide-rich peptides, 2 mM EDTA was added during the 1 h induction. Bacteria were then washed with PBS containing 10 mM $MgCl_2$ to improve membrane stability.

Oxidative Folding of Synthesized Peptides. Acyclic kalata B1 variants were prepared using solid phase peptide synthesis and oxidatively folded in solution. Reduced peptides (Selleck Chemicals) at 5 mg mL^{-1} in 30 mM Tris (pH 7.4) with 50% v/v acetonitrile were added to 166 mg of ClearOx (Peptides International) and incubated at RT for 24 h. The reaction mixture was purified by RP-HPLC on a C18 column using a gradient of 1.28% acetonitrile min^{-1}. The collected fractions were analyzed with ESI-TOF mass spectrometry and verified to possess the expected molecular weight and three disulfide bonds. Cyclic kalata B1 variants were prepared by folding synthetically produced peptides (0.25 mg mL^{-1}) in 0.1 M ammonium bicarbonate (pH 8.3) with 2 mM TCEP for 24 h at RT and purified by RP-HPLC.

Measuring Affinities Using SPR. The binding kinetics of synthetic peptides were measured by SPR using a Biacore 3000. Peptide concentrations in HBS buffer were measured by BCA. Human and mouse NRP1, and human NRP2 (R&D Systems) (20 μg mL^{-1} in acetate buffer, pH 4) were immobilized to 2300, 3100, and 5000 RU, respectively, on a CM4 chip using NHS/EDC and capped with ethanolamine; a CM4 chip was used to reduce non-specific electrostatic interactions. A 3-fold dilution series of peptide (4 nM–1 μM) was injected at 50 μL min^{-1} in HBS-EP (10 mM HEPES, pH 7.4, 150 mM NaCl, 3 mM EDTA, and 0.05% v/v Tween 20). The surface was regenerated using 5 μL of 10 mM HCl. For analysis, the binding responses were double-referenced to a blank flow cell and a buffer injection.

MTT Assay To Measure Peptide Cytotoxicity. Peptide cytotoxicity assays were performed with PPC-1, M21, and MDA-MB-231 cell lines with 0.4, 2, and 10 μM peptide. Cells were seeded into 96-well plates and incubated for 24 h at 37 °C. The peptides were diluted into DMEM with 10% v/v FBS, and 100 μL of peptide solution was added to each well and incubated for 24 h. MTT reagent was then added according to the manufacturer's instructions. As a positive control for toxicity, melittin, the major component of bee venom (GIGAVLKVLTTGLPALISWIKRKRQQ-NH_2, Anaspec), was tested with a 5-fold concentration series from 80 nM to 50 μM.

Transwell Migration Assays and HUVEC Viability. HUVECs (Lonza) were grown to confluency in EGM-2 with 5% v/v FBS and then serum-starved in the assay medium (EBM-2 with 0.1% v/v FBS) for 16 h. Transwell inserts (8 μM pores, Millipore) were coated with attachment factor (Gibco), and 100,000 HUVECs were seeded per insert. The peptide was added to the top of the insert and incubated for 45 min at 37 °C prior to the addition of 3.3 nM $VEGFA_{165}$ to the bottom chamber. Cells were allowed to migrate for an additional 5 h and fixed using paraformaldehyde, stained with DAPI, and counted across 10 fields of view using a 40x objective.

To determine whether peptides were cytotoxic to HUVECs under the migration conditions, cells were serum-starved and seeded into a 96-well plate precoated with attachment factor (30,000 cells per well). Cells were incubated with peptides for 6 h at 37 °C, and then 10% v/v alamarBlue was added to each well to incubate for an additional 1 h prior to measuring the fluorescence (excitation 540 nm, emission 590 nm).

Protease Stability via LC–MS. Cyclic kalata B1, acyclic N2.1, and cyclic N2.1C at a final concentration of 0.3 mg mL^{-1} were incubated with either 200 nM uPA, 200 nM MMP-9, or 20 nM MT-SP1 (R&D Systems) at 37 °C for 6 h. The samples were analyzed via LC–MS, and the extent of degradation was measured using the integrated area of the 220 nm absorbance peaks.

■ ASSOCIATED CONTENT

Supporting Information

This material is available free of charge via the Internet at http://pubs.acs.org.

■ AUTHOR INFORMATION

Corresponding Author

*E-mail: psd@engineering.ucsb.edu.

Notes

The authors declare no competing financial interest.

■ ACKNOWLEDGMENTS

This work was supported by U.S. Army Research Office-Institute for Collaborative Biotechnologies grants DAAD19-03-D-0004 and W911NF-09-D-0001. D.J.C. is grateful for the support of a National Health and Medical Research Council (Australia) Professorial Fellowship and grant (APP1026501 and APP1028509). We thank S. Lanati for her advice on the HUVEC migration assay.

■ REFERENCES

(1) Rizzolio, S., and Tamagnone, L. (2011) Multifaceted role of neuropilins in cancer. *Curr. Med. Chem. 18*, 3563–3575.

(2) Soker, S., Fidder, H., Neufeld, G., and Klagsbrun, M. (1996) Characterization of novel vascular endothelial growth factor (VEGF) receptors on tumor cells that bind VEGF via its exon 7-encoded domain. *J. Biol. Chem. 271*, 5761–5767.

(3) Soker, S., Takashima, S., Miao, H. Q., Neufeld, G., and Klagsbrun, M. (1998) Neuropilin-1 is expressed by endothelial and tumor cells as an isoform-specific receptor for vascular endothelial growth factor. *Cell 92*, 735–745.

(4) Bachelder, R. E., Crago, A., Chung, J., Wendt, M. A., Shaw, L. M., Robinson, G., and Mercurio, A. M. (2001) Vascular endothelial growth factor is an autocrine survival factor for neuropilin-expressing breast carcinoma cells. *Cancer Res. 61*, 5736–5740.

(5) Hu, B., Guo, P., Bar-Joseph, I., Imanishi, Y., Jarzynka, M. J., Bogler, O., Mikkelsen, T., Hirose, T., Nishikawa, R., and Cheng, S. Y. (2007) Neuropilin-1 promotes human glioma progression through potentiating the activity of the HGF/SF autocrine pathway. *Oncogene 26*, 5577–5586.

(6) Ochiumi, T., Kitadai, Y., Tanaka, S., Akagi, M., Yoshihara, M., and Chayama, K. (2006) Neuropilin-1 is involved in regulation of apoptosis and migration of human colon cancer. *Int. J. Oncol. 29*, 105–116.

(7) Wey, J. S., Gray, M. J., Fan, F., Belcheva, A., McCarty, M. F., Stoeltzing, O., Somcio, R., Liu, W., Evans, D. B., Klagsbrun, M., Gallick, G. E., and Ellis, L. M. (2005) Overexpression of neuropilin-1 promotes constitutive MAPK signalling and chemoresistance in pancreatic cancer cells. *Br. J. Cancer 93*, 233–241.

(8) Matsushita, A., Götze, T., and Korc, M. (2007) Hepatocyte growth factor-mediated cell invasion in pancreatic cancer cells is dependent on neuropilin-1. *Cancer Res. 67*, 10309–10316.

(9) Rizzolio, S., Rabinoviz, N., Rainero, E., Lanzetti, L., Serini, G., Norman, J. C., Neufeld, G., and Tamagnone, L. (2012) Neuropilin-1 dependent regulation of EGF-Receptor signaling. *Cancer Res. 17*, 5801−5811.
(10) Pan, Q., Chanthery, Y., Liang, W.-C., Stawicki, S., Mak, J., Rathore, N., Tong, R. K., Kowalski, J., Yee, S. F., Pacheco, G., Ross, S., Cheng, Z., Le Couter, J., Plowman, G., Peale, F., Koch, A. W., Wu, Y., Bagri, A., Tessier-Lavigne, M., and Watts, R. J. (2007) Blocking neuropilin-1 function has an additive effect with anti-VEGF to inhibit tumor growth. *Cancer Cell 11*, 53−67.
(11) Xin, Y., Bai, S., Damico-Beyer, L., Jin, D., Liang, W.-C., Wu, Y., Theil, F.-P., Joshi, A., Lu, Y., Lowe, J., Maia, M., Brachmann, R., and Xiang, H. (2012) Anti-neuropilin-1 (MNRP1685A): Unexpected pharmacokinetic differences across species, from preclinical models to humans. *Pharm. Res. 29*, 2512−2521.
(12) Bumbaca, D., Xiang, H., Boswell, C. A., Port, R. E., Stainton, S. L., Mundo, E. E., Ulufatu, S., Bagri, A., Theil, F.-P., Fielder, P. J., Khawli, L. A., and Shen, B.-Q. (2012) Maximizing tumour exposure to anti-neuropilin-1 antibody requires saturation of non-tumour tissue antigenic sinks in mice. *Br. J. Pharmacol. 166*, 368−377.
(13) Sugahara, K. N., Teesalu, T., Karmali, P. P., Kotamraju, V. R., Agemy, L., Greenwald, D. R., and Ruoslahti, E. (2010) Coadministration of a tumor-penetrating peptide enhances the efficacy of cancer drugs. *Science 328*, 1031−1035.
(14) Sugahara, K. N., Teesalu, T., Karmali, P. P., Kotamraju, V. R., Agemy, L., Girard, O. M., Hanahan, D., Mattrey, R. F., and Ruoslahti, E. (2009) Tissue-penetrating delivery of compounds and nanoparticles into tumors. *Cancer Cell 16*, 510−520.
(15) Caunt, M., Mak, J., Liang, W.-C., Stawicki, S., Pan, Q., Tong, R. K., Kowalski, J., Ho, C., Reslan, H. B., Ross, J., Berry, L., Kasman, I., Zlot, C., Cheng, Z., Le Couter, J., Filvaroff, E. H., Plowman, G., Peale, F., French, D., Carano, R., Koch, A. W., Wu, Y., Watts, R. J., Tessier-Lavigne, M., and Bagri, A. (2008) Blocking neuropilin-2 function inhibits tumor cell metastasis. *Cancer Cell 13*, 331−342.
(16) Čemažar, M., and Craik, D. (2006) Factors influencing the stability of cyclotides: proteins with a circular backbone and cystine knot motif. *Int. J. Pept. Res. Ther. 12*, 253−260.
(17) Getz, J. A., Rice, J. J., and Daugherty, P. S. (2011) Protease-resistant peptide ligands from a knottin scaffold library. *ACS Chem. Biol. 6*, 837−844.
(18) Wong, C. T. T., Rowlands, D. K., Wong, C.-H., Lo, T. W. C., Nguyen, G. K. T., Li, H.-Y., and Tam, J. P. (2012) Orally active peptidic bradykinin B1 receptor antagonists engineered from a cyclotide scaffold for inflammatory pain treatment. *Angew. Chem., Int. Ed. 124*, 5718−5722.
(19) Eliasen, R., Daly, N. L., Wulff, B. S., Andresen, T. L., Conde-Frieboes, K. W., and Craik, D. J. (2012) Design, synthesis, structural and functional characterization of novel melanocortin agonists based on the cyclotide kalata B1. *J. Biol. Chem. 287*, 40493−40501.
(20) Haspel, N., Zanuy, D., Nussinov, R., Teesalu, T., Ruoslahti, E., and Aleman, C. (2011) Binding of a C-end rule peptide to the neuropilin-1 receptor: a molecular modeling approach. *Biochemistry 50*, 1755−1762.
(21) He, Z., and Tessier-Lavigne, M. (1997) Neuropilin is a receptor for the axonal chemorepellent semaphorin III. *Cell 90*, 739−751.
(22) Teesalu, T., Sugahara, K. N., Kotamraju, V. R., and Ruoslahti, E. (2009) C-end rule peptides mediate neuropilin-1-dependent cell, vascular, and tissue penetration. *Proc. Natl. Acad. Sci. U.S.A. 106*, 16157−16162.
(23) Claffey, K. P., Brown, L. F., Del Aguila, L. F., Tognazzi, K., Yeo, K.-T., Manseau, E. J., and Dvorak, H. F. (1996) Expression of vascular permeability factor/vascular endothelial growth factor by melanoma cells increases tumor growth, angiogenesis, and experimental metastasis. *Cancer Res. 56*, 172−181.
(24) Roth, L., Agemy, L., Kotamraju, V. R., Braun, G., Teesalu, T., Sugahara, K. N., Hamzah, J., and Ruoslahti, E. (2011) Transtumoral targeting enabled by a novel neuropilin-binding peptide. *Oncogene 31*, 3754−3763.
(25) Daly, N. L., Love, S., Alewood, P. F., and Craik, D. J. (1999) Chemical synthesis and folding pathways of large cyclic polypeptides: studies of the cystine knot polypeptide kalata B1. *Biochemistry 38*, 10606−10614.
(26) Liang, W.-C., Dennis, M. S., Stawicki, S., Chanthery, Y., Pan, Q., Chen, Y., Eigenbrot, C., Yin, J., Koch, A. W., Wu, X., Ferrara, N., Bagri, A., Tessier-Lavigne, M., Watts, R. J., and Wu, Y. (2007) Function blocking antibodies to neuropilin-1 generated from a designed human synthetic antibody phage library. *J. Mol. Biol. 366*, 815−829.
(27) Gruber, C. W., Čemažar, M., Clark, R. J., Horibe, T., Renda, R. F., Anderson, M. A., and Craik, D. J. (2007) A novel plant protein-disulfide isomerase involved in the oxidative folding of cystine knot defense proteins. *J. Biol. Chem. 282*, 20435−20446.
(28) Parker, M. W., Xu, P., Li, X., and Vander Kooi, C. W. (2012) Structural basis for the selective vascular endothelial growth factor-A (VEGF-A) binding to neuropilin-1. *J. Biol. Chem. 287*, 11082−11089.
(29) Soman, N. R., Baldwin, S. L., Hu, G., Marsh, J. N., Lanza, G. M., Heuser, J. E., Arbeit, J. M., Wickline, S. A., and Schlesinger, P. H. (2009) Molecularly targeted nanocarriers deliver the cytolytic peptide melittin specifically to tumor cells in mice, reducing tumor growth. *J. Clin. Invest. 119*, 2830−2842.
(30) Cascales, L., Henriques, S. T., Kerr, M. C., Huang, Y.-H., Sweet, M. J., Daly, N. L., and Craik, D. J. (2011) Identification and characterization of a new family of cell-penetrating peptides. *J. Biol. Chem. 286*, 36932−36943.
(31) Owen, K. A., Qiu, D., Alves, J., Schumacher, A. M., Kilpatrick, L. M., Li, J., Harris, J. L., and Ellis, V. (2010) Pericellular activation of hepatocyte growth factor by the transmembrane serine proteases matriptase and hepsin, but not by the membrane-associated protease uPA. *Biochem. J. 426*, 219−228.
(32) Kong, D., Li, Y., Wang, Z., Banerjee, S., and Sarkar, F. H. (2007) Inhibition of angiogenesis and invasion by 3,3′-diindolylmethane is mediated by the nuclear factor-κB downstream target genes MMP-9 and uPA that regulated bioavailability of vascular endothelial growth factor in prostate cancer. *Cancer Res. 67*, 3310−3319.
(33) Bajou, K., Lewalle, J.-M., Martinez, C. R., Soria, C., Lu, H., Noël, A., and Foidart, J.-M. (2002) Human breast adenocarcinoma cell lines promote angiogenesis by providing cells with uPA-PAI-1 and by enhancing their expression. *Int. J. Cancer 100*, 501−506.
(34) Taraboletti, G., D'Ascenzo, S., Borsotti, P., Giavazzi, R., Pavan, A., and Dolo, V. (2002) Shedding of the matrix metalloproteinases MMP-2, MMP-9, and MT1-MMP as membrane vesicle-associated components by endothelial cells. *Am. J. Pathol. 160*, 673−680.
(35) Jia, H., Bagherzadeh, A., Hartzoulakis, B., Jarvis, A., Löhr, M., Shaikh, S., Aqil, R., Cheng, L., Tickner, M., Esposito, D., Harris, R., Driscoll, P. C., Selwood, D. L., and Zachary, I. C. (2006) Characterization of a bicyclic peptide neuropilin-1 (NP-1) antagonist (EG3287) reveals importance of vascular endothelial growth factor exon 8 for NP-1 binding and role of NP-1 in KDR signaling. *J. Biol. Chem. 281*, 13493−13502.
(36) Kenrick, S., Rice, J., and Daugherty, P. (2007) Flow cytometric sorting of bacterial surface-displayed libraries. *Curr. Protoc. Cytom. 42*, 4.6.1−4.6.27.
(37) Dane, K. Y., Gottstein, C., and Daugherty, P. S. (2009) Cell surface profiling with peptide libraries yields ligand arrays that classify breast tumor subtypes. *Mol. Cancer Ther. 8*, 1312−1318.
(38) Getz, J. A., Schoep, T. S., and Daugherty, P. S. (2012) Peptide discovery using bacterial display and flow cytometry, in *Methods in Enzymology: Protein Engineering for Therapeutics, Part A* (Wittrup, K. D., Ed.) 1st ed., pp 75−97, Academic Press, San Diego, CA.
(39) Giebel, L. B., Cass, R., Milligan, D. L., Young, D., Arze, R., and Johnson, C. (1995) Screening of cyclic peptide phage libraries identifies ligands that bind streptavidin with high affinities. *Biochemistry 34*, 15430−15435.